Eur. Phys. J. Special Topics **223**, 1895–1906 (2014)

DOI: 10.1140/epjst/e2014-02234-7

THE EUROPEAN PHYSICAL JOURNAL SPECIAL TOPICS

Regular Article

Competition between anisotropic viscous fingers

M. Pecelerowicz, A. Budek, and P. Szymczak[a]

Institute of Theoretical Physics, Faculty of Physics, University of Warsaw, Hoza 69, 00-681 Warsaw, Poland

Received 30 June 2014 / Received in final form 21 July 2014
Published online 22 September 2014

Abstract. We consider viscous fingers created by injection of low viscosity fluid into the network of capillaries initially filled with a more viscous fluid (motor oil). Due to the anisotropy of the system and its geometry, such a setup promotes the formation of long-and-thin fingers which then grow and compete for the available flow, interacting through the pressure field. The interaction between the fingers is analyzed using the branched growth formalism of Halsey and Leibig (Phys. Rev. A **46**, 7723, 1992) using a number of simple, analytically tractable models. It is shown that as soon as the fingers are allowed to capture the flow from one another, the fixed point appears in the phase space, corresponding to the asymptotic state in which the growth of one of the fingers in hindered by the other. The properties of phase space flows in such systems are shown to be remarkably insensitive to the details of the dynamics.

1 Introduction

Unstable growth phenomena are one of the most common pattern-forming processes in nature. Alas, although in many cases the physical laws governing a particular growth process are well-understood, the highly non-local character of interface dynamics makes the problem elusive for an analytical treatment. Within few exceptions, rigorous results are limited to the early stages of the growth, when linear approximation can be used. In that way one can get the growth rates and wavelengths of the initial instability which leads to the appearance of small corrugations on the interface. With time, these corrugations grow and transform themselves into fingers, dendrites, bubbles or disordered, fractal structures. These nonequilibrium structures interact with each other in a strongly nonlinear way, which gives rise to a complex dynamics of the front, particularly challenging to analyze. For example, in miscible fingering problem [1,2], the emerging fingers are incessantly merging, fading, shielding, and tip splitting [3–5], but no detailed quantitative characterization of this nonlinear dynamics has been provided yet.

In order to get at least partial understanding of the nonlinear dynamics of advancing front it is advantageous to consider a system in which the interactions between

[a] e-mail: Piotr.Szymczak@fuw.edu.pl

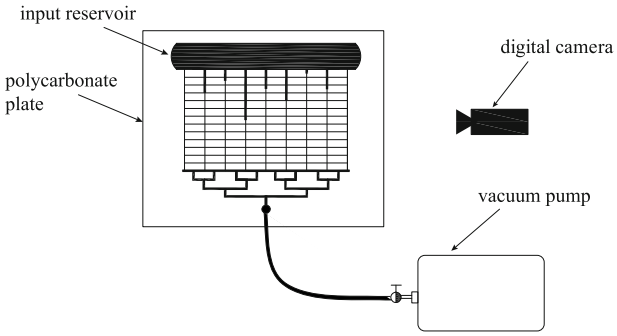

Fig. 1. Schematic representation of the experimental set-up [6]. A lower viscosity fluid is injected along upper surface into a rectangular network of capillaries, initially filled with a higher viscosity fluid (motor oil). The size of the plate is 6.5×6.5 cm and the cross sections of capillaries are $400\,\mu\text{m} \times 400\,\mu\text{m}$. Additionally, the upstream part of the plate is milled to accommodate $5.5\,\text{cm} \times 0.5\,\text{cm} \times 0.25\,\text{cm}$ input reservoir space. The downstream part is milled to accommodate a hierarchical system of outlet channels, connected to the vacuum pump. Such a setup helps in keeping the uniform pressure along the downstream edge of the network.

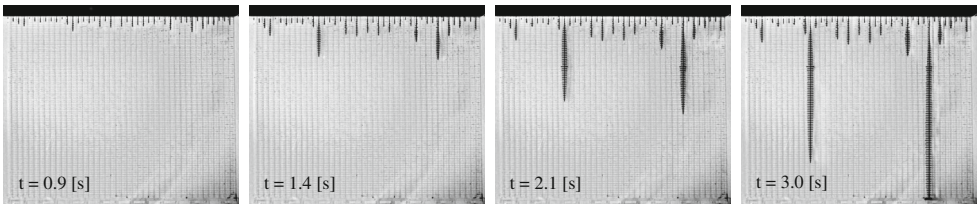

Fig. 2. The evolution of the finger patterns during the injection of water (dyed with ink, hence the dark color) into the network filled with motor oil of viscosity $\mu \approx 0.5\,\text{Pas}$.

the fingers is forced to be simpler. With this in mind, we have conducted a series of viscous fingering experiments in a network of microfluidic channels, milled in polycarbonate plates [6]. As illustrated in Fig. 1, a lower viscosity fluid (water dyed with ink) was pushed into a rectangular grid of channels, initially filled with a higher viscosity fluid.

The presence of the underlying lattice promotes the growth of long-and-thin fingers, oriented along the pressure drop direction. In Fig. 2, the finger patterns captured at different times are shown. As observed, the dynamics of the fingers is highly selective: at the beginning many short fingers appear, but the growth of most of them is soon stopped and only a few continue to grow. The selection process then repeats itself which results in a distance between active (growing) fingers increasing in time. Such a self-similar selection process usually results in a scale-free distribution of finger lengths:

$$N(L) \sim L^{-m}, \tag{1}$$

where $N(L)$ is the number of finger longer than L and m is the exponent of the power law. Experiments on viscous fingering in channel networks had been performed previously [7–10], however in a radial geometry, which makes the analysis of finger-finger interaction and competition less straightforward, since the effective distance between radially growing fingers increases in time.

The nature of the interaction between the fingers underlying the selection process may be understood by analyzing the flow of the invading and displaced fluid in

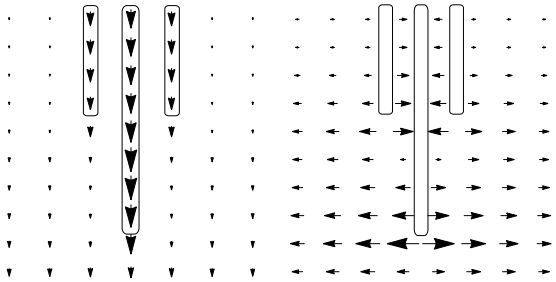

Fig. 3. The flow around a longer finger (in the centre) flanked by the two shorter ones. The panels on the left show the flow in the vertical channels, the panels on the right – in the horizontal ones.

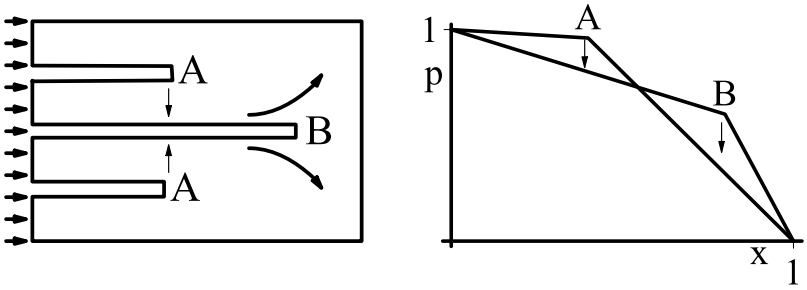

Fig. 4. A schematic view of a long finger with the two shorter neighbors (left) and the corresponding pressure drops along the long finger and one of the shorter ones (right). Since the pressure gradient in the longer finger is steeper than in the shorter one, the flow lines are converging towards a longer finger in the upstream part and diverging from it near the finger tip.

between the growing fingers. Figure 3 presents the flow patterns in the vicinity of a longer finger flanked by two shorter ones. A characteristic "converging-diverging" pattern is observed there, with the flow directed towards the longer channel in the upstream part and outwards from the main channel in the downstream part. The origin of such a pattern can be elucidated by analyzing the pressure drops in the fingers, as shown schematically in Fig. 4. Since there is a constant pressure drop between the inlet and outlet, the pressure gradient in the longer finger will be steeper than in the shorter one; this is because the flow rate is higher in the long finger. In the upstream part of the system, the short finger is at a higher pressure than the long one, so the flow is directed toward the long finger. Downstream, the region around the tip of the long finger is at a higher pressure than the surrounding network hence the flow is directed away from the finger, resulting in the flow pattern observed in Fig. 3. Such a "converging-diverging" flow pattern is a characteristic feature of the fingered growth systems, also observed in the growth of wormholes in dissolving porous rock [11,12]. This is the way the fingers interact: the flow is sucked from the shorter finger towards the longer one. Importantly, the larger the difference in finger lengths, the higher the pressure drop between the fingers. Since the larger flow in the finger leads to its faster growth, this generates a positive feedback loop resulting in fast growth of the longer fingers and starvation of the shorter ones.

The aim of this paper is to investigate the competition process in a quantitative way, by considering a number of simple models of the finger growth and interaction, inspired by the experimental observations. We will limit ourselves to the pair of competing fingers, leaving the $n-$finger case for the further study. In Sect. 2 we

introduce the phase space description of the finger dynamics, originally by Halsey and Leibig. This is the basic tool used throughout the paper to analyze the competition between the fingers. Next, in Sect. 3 we consider the case of two independently growing fingers, which allows us to gain insight into the structure of the flow in the phase space. Then, in Sect. 4, we introduce the simplest possible model of the interaction between the fingers, connecting them with two capillaries which allow for the exchange of the flow between them. Finally, in Sect. 5 we consider a more realistic system: two thin fingers formed of a lower viscosity fluid invading a 2d-system initially filled with a higher viscosity fluid, which can be seen as a continuous version of the experimental system of Fig. 2.

Although the direct inspiration for this study was the viscous fingering system described above, we believe that the models presented here can also be used to describe the interaction between the fingers in similar systems, such as a "racetrack" for viscous fingers [13], the competition between the branching viscous fingers [14] or side-branch growth in solidifying dendrites [15,16].

2 Two-finger phase-space

As proposed by Halsey and Leibig [17], originally in the context of diffusion-limited aggregation, the competition between two growing fingers can be conveniently analyzed in the variables

$$x = \frac{v_A}{v_A + v_B} \qquad y = \frac{L_A}{L_A + L_B}, \tag{2}$$

where L_i are the lengths of the fingers and v_i – their growth rates. As observed in [17], the evolution equation for y takes a particularly simple form when the time is measured by the logarithm of the total length of the fingers, $L = L_A + L_B$. In such case, we get

$$\frac{dy}{d\log L} = L\frac{dy}{dL} = \frac{dL_A}{dL} - \frac{L_A}{L} = x - y. \tag{3}$$

The dynamics should now be supplemented with the analogous equation for the evolution of x, namely

$$\frac{dx}{d\log L} = G(x, y). \tag{4}$$

However, the function $G(x, y)$ is generally hard to find. For the case of DLA in 2d it was constructed with the use of renormalization group techniques (in the mean-field approximation) in [18]. Even if the exact form of $G(x, y)$ is unknown, it is still possible to explore a number of properties of dynamics in (x, y) space using the symmetry arguments. For example, interchanging indices A and B leads to $G(x, y) = -G(1-x, 1-y)$. Next, one notices that, by symmetry, the point $C = (\frac{1}{2}, \frac{1}{2})$ is a fixed point of the dynamics, thus $G(\frac{1}{2}, \frac{1}{2}) = 0$. This corresponds to the case where both fingers have equal length. Other potential fixed points are $D_1 = (0, 0)$ and $D_2 = (1, 1)$ which correspond to the cases where finger B (or A) has won the competition completely. Because of the above symmetries, and since the longer finger always grows faster than the shorter one, the complete information on the dynamics of the system is contained in $0 \le x \le 1/2,\ 0 \le y \le 1/2$ portion of the phase space, which corresponds to the assumption that finger A is the shorter of the two.

The presence of fixed points and their stability are the key factors governing the dynamics of the fingers. In particular, there are two physically distinct regimes: a stable C point together with unstable D points corresponds to the case when two

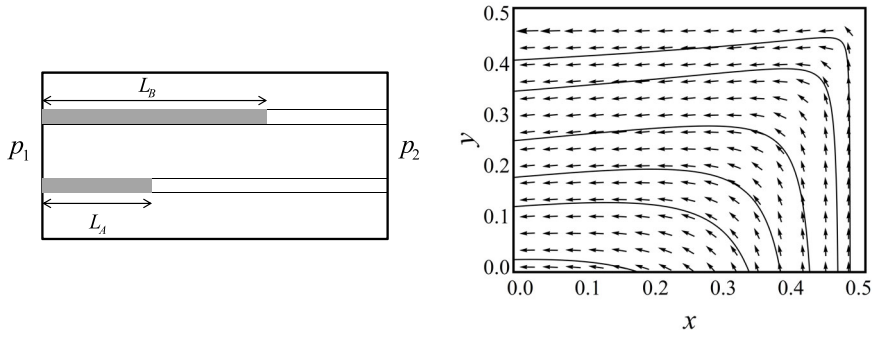

Fig. 5. Left: displacing a higher viscosity fluid (white) with a lower viscosity one (dark) in two independent fingers. Right: the corresponding phase space trajectories.

fingers, no matter how unequal at the beginning, always asymptotically approach a state in which they become perfectly equal. This corresponds to the growth processes with "dense branched morphology" [19]. Here, we are interested in another regime, in which C point is unstable whereas D is stable. In other words, any difference in length between the fingers will be eventually amplified by the dynamics and the growth of the shorter finger will be hindered by the longer one.

3 Two independent fingers

First, as a trivial yet instructive example, the case of two independently evolving fingers is considered. The simplest setup of this kind consists of two identical parallel capillaries initially filled with a more viscous fluid, into which – just as in the standard viscous fingering experiment – a lower viscosity fluid is injected under the imposed pressure drop, $\Delta p = p_1 - p_2$ (*cf.* Fig. 5). The volumetric flow rates in the capillaries are then

$$q_A = \frac{p_1 - p_2}{L_A\rho_1 + (L_0 - L_A)\rho_2} \qquad q_B = \frac{p_1 - p_2}{L_B\rho_1 + (L_0 - L_B)\rho_2}, \tag{5}$$

where L_0 is the total length of the system and ρ_1 and ρ_2 are the hydraulic resistivities of the capillary filled with a lower and higher viscosity fluid respectively. For a cylindrical capillary:

$$\rho_i = \frac{\pi r^4}{8\eta_i} \tag{6}$$

where r is the capillary radius. We assume that the finger moves with the velocity corresponding to the mean flow rate in the capillary, i.e.

$$v_i = \frac{q_i}{s} \tag{7}$$

where s is the cross-sectional area of the capillary.

For the phase-space evolution, a simple algebra gives in this case

$$\frac{dx}{d\log L} = \frac{(1-2x)^2}{2y-1}, \qquad x \le \frac{1}{2}, y \le \frac{1}{2}\,. \tag{8}$$

Note that the resulting evolution equation is very simple and completely independent of the resistivities ρ_1 and ρ_2. Although they are important if the finger length evolution

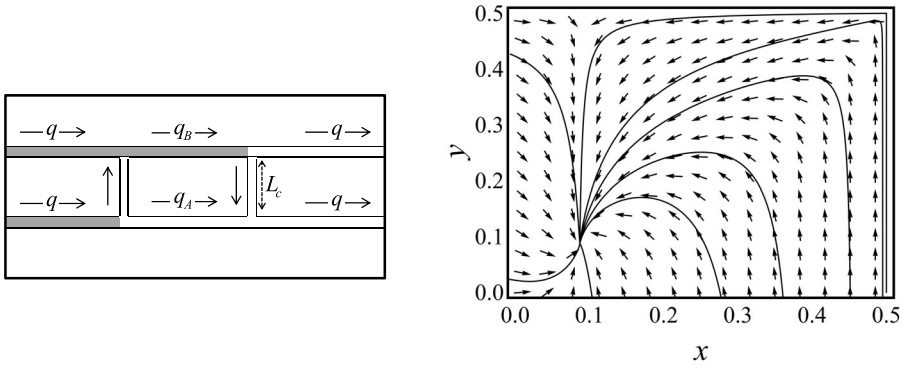

Fig. 6. Left: a simple model of finger-finger interactions: the fingers are connected with two capillaries of length L_c, one positioned at the tip of the shorter finger and the other – at the tip of the longer one. Right: the corresponding phase space trajectories.

in time, $L_A(t)$ and $L_B(t)$, is of interest, they have no impact on the xy trajectories, which shows that this choice of the phase space variables indeed leads to the significant simplifications in the description of the system. Moreover, the phase space dynamics remains the same if the constant pressure drop condition is replaced by a constant total flow one ($q_A + q_B = const$).

The phase space trajectories are presented in the right panel of Fig. 5. Let us note that the fixed point $C = (1/2, 1/2)$ is singular. It may be classified as unstable, though, since the points in its neighborhood of C eventually drift away from it. Also, the point (0,0) is not a fixed point of the dynamics, which is caused by the fact that the fingers evolve independently. The flow capturing mechanism is not present here and both fingers remain active throughout their whole evolution. Another important point to keep in mind here is that the constraint that $L_A, L_B < L_0$ means that each trajectory terminates at a specific point in the phase space, corresponding to the time at which the longer finger reaches the outlet of the system.

Although trivial, the above considered case is nevertheless insightful. In particular, as it will be shown below, the term $\frac{(1-2x)^2}{2y-1}$ derived above is present also in the evolution equations in more complicated cases of interacting fingers.

4 Two fingers interacting via connectors

Next, following [20], we introduce a simple model of an interaction between the fingers. As it has already been mentioned the flow around the fingers has a characteristic "converging-diverging" pattern with the flow velocity directed towards the longer finger near the tip of the shorter one and outwards from the longer finger near its tip. The simplest network which would allow such a flow pattern can be obtained by adding two connectors between the capillaries – one at the tip of the shorter finger and the other – at the tip of the longer one, as illustrated in Fig. 6. Taken literally, this would require that the connectors change their position in the system as the fingers grow; however one should rather see it as a model of many-connector case in which we neglect the flow in all the connectors except for those located near the finger tips, where the flow magnitude is expected to be the strongest. Such a model was introduced in [20] to track the dynamics of the wormhole-like channels in a dissolving rock fracture and has proved to be successful in predicting the length distribution of the wormholes.

In [20] a constant pressure drop condition was imposed at the end of the system. Here, however, in order to keep the algebra simple we will impose the condition of a fixed pressure gradient (and hence fixed flow) both at the upstream and the downstream part of the sample ($q = const.$ in Fig. 6).

We assume that the speeds of advancement of the fingers are proportional to the velocity of the fluid in the channel directly overhead, i.e.

$$\frac{dL_B}{dt} = q/s, \qquad \frac{dL_A}{dt} = q_A/s, \tag{9}$$

according to the notation in Fig. 6. The flow q_A can be solved for in a straightforward manner and reads

$$q_A = 2q\frac{(L_B - L_A)\rho_1 + L_c\rho_2}{(L_B - L_A)(\rho_1 + \rho_2) + 2L_c\rho_2}, \tag{10}$$

where L_c is the length of the connecting capillaries. For the phase-space dynamics we get in this case

$$\frac{dx}{d\log L} = \frac{(1-2x)^2((3x-2)\rho_1 + x\rho_2)}{(2y-1)(\rho_2 - \rho_1)}, \qquad x \leq \frac{1}{2}, y < \frac{1}{2} \tag{11}$$

with the corresponding trajectories given in the right panel of Fig. 6. A notable feature of the phase-space in this case is the appearance of a stable fixed point with the coordinates

$$x_f = y_f = \frac{2\rho_1}{3\rho_1 + \rho_2}\,. \tag{12}$$

The fixed point is different from $(0, 0)$, which shows that the longer finger screens the shorter one only partially. Indeed, even if the entire capillary A is filled with the higher viscosity fluid, and B – with the lower viscosity one, the ratio of hydraulic resistances between these two flow paths remains finite, which results in the finite value of v_A/v_B in the long-time limit.

The Jacobian matrix at the fixed point reads

$$\begin{pmatrix} -1 & 0 \\ 1 & -1 \end{pmatrix},$$

with a single, defective eigenvalue (-1) and a corresponding eigenvector $\eta = (0, 1)$. The fixed point at $(0, 0)$ is thus a stable improper node.

Note that the above dynamics is completely independent of the length of the connector L_c. This means that even if initially the channels were separated by a large distance, eventually they will feel each other and the flow of one of them will be captured by the other. Naturally, the further they are from each other, the more time it takes for the interaction to become important, but its character does not change. It is precisely the invariant character of the finger-finger interaction that leads to the appearance of self-similar structure as in Fig. 2.

In this simple case, it is even possible to integrate directly the equations of motion getting

$$L_B(t) = L_B(t=0) + \frac{q}{s}t \tag{13}$$

$$L_A(t) = L_B(t) - \frac{2L_c\rho_2}{\rho_1 + \rho_2}W(Ce^{\frac{qt}{2L_c s\rho_2}(\rho_2 - \rho_1)}). \tag{14}$$

Here W is the Lambert W function, defined as the solution of the equation $W(z)e^{W(z)} = z$ and C is the constant to be determined from the initial condition.

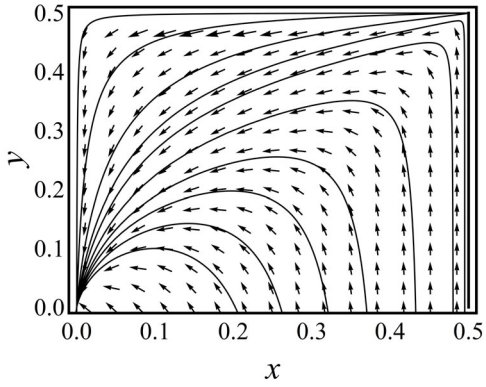

Fig. 7. The phase space flow for the case of the interacting fingers of Fig. 6 in the limit of the infinite viscosity ratio.

It is of interest to consider the limit of infinite viscosity ratio, i.e. $\rho_2/\rho_1 \to \infty$. In that limit

$$\frac{dx}{d\log L} = \frac{x(1-2x)^2}{2y-1}, \qquad x < \frac{1}{2},\ y \leq \frac{1}{2} \tag{15}$$

with the corresponding phase space dynamics given in Fig. 7. This expression contains the same two terms as in the case of independent fingers (8) and, additionally, an extra "x" term. It is the presence of this term which leads to the appearance of the stable node, which in this case is $(0, 0)$, corresponding to the situation where the whole flow is focused in the stronger finger.

Application of the infinite viscosity ratio limit leads also to the simplifications in Eq. (14):

$$L_A = L_B - 2L_c W(Ce^{\frac{qt}{2L_c s}}). \tag{16}$$

In the long-time limit this behaves asymptotically as

$$L_A \approx 2L_c \log \frac{qt}{2L_c s}, \tag{17}$$

where the asymptotics of the Lambert function. $W(z) \approx \log z - \log\log z$ has been used. Thus the shorter finger grows logarithmically in time, whereas the longer finger grows with a constant growth rate. Note that although also in this case the shorter finger never completely ceases to grow, for long times its growth rate is negligible in comparison with the longer one and the ratio of lengths of the two fingers goes to zero.

5 Two finger system – thin finger formalism

Finally, we consider a more realistic system in which two straight, thin fingers of lower viscosity fluid penetrate a rectangular cell initially filled with a higher viscosity fluid. This can be looked upon as a continuous version of the experimental system of Fig. 1. In order to render the problem analytically tractable, we assume that the fingers are infinitely thin, i.e. they can be approximated by the line segments, and we adopt the limit of infinite viscosity ratio, i.e. $\rho_2/\rho_1 \to \infty$, as well as the periodic boundary conditions at the side walls. A schematic of the system is presented in the left panel of Fig. 8. The fingers grow vertically upwards in a rectangular cell of width W with

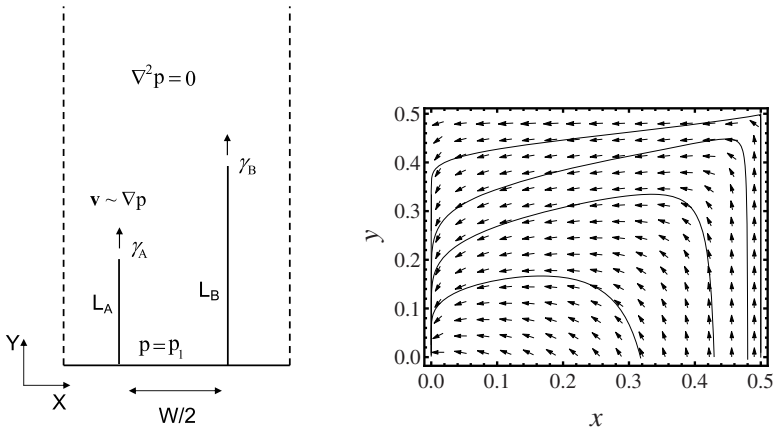

Fig. 8. Two Laplacian fingers growing in a rectangular cell in periodic boundary conditions (left) and the corresponding phase space diagram (right).

periodic boundary conditions in lateral (X) direction. The pressure field outside the fingers (in a more viscous liquid) is the solution of the Laplace equation, $\nabla^2 p = 0$. Additionally, the Dirichlet boundary conditions for the pressure ($p = p_1$) are imposed both on the fingers and the bottom wall ($Y = 0$), whereas $\frac{\partial p}{\partial Y} \xrightarrow[y\to\infty]{} 1$ (constant flux at infinity). Subsequently it will prove more convenient to subtract p_1 from the pressure, i.e. work with $p' = p - p_1$, as this function vanishes on the fingers and the bottom wall.

The growth rates of the fingers should be proportional to the pressure gradients near their tips. However, since the finger is assumed to be infinitely thin, there is a singularity in a field gradient at its tip. Namely, at a small distance r from the tip of ith finger, the pressure takes the form

$$p_i'(\mathbf{r}, t) = C_i(t)\sqrt{r}\cos(\theta/2), \tag{18}$$

where the coefficients $C_i(t)$ depend on lengths and shapes of all the fingers. In the above, the origin of coordinates is located at the tip of the finger and the polar axis is directed along it. The pressure gradient will then have $r^{-1/2}$ singularity. In actual experimental system this singularity is removed, since the pressure gradient in each elementary channel comprising the network is approximately constant. The velocity of a real finger is then well approximated by:

$$v_i = \frac{C_i(t)}{\rho_1 s\sqrt{l}}, \tag{19}$$

where l is the length of the elementary channel in the network.

The pressure field around the fingers can be calculated using conformal mapping techniques, as shown in [21]. First, the mapping

$$w(z) = \frac{-\cosh\left(\frac{2L_A\pi}{W}\right) + \cosh\left(\frac{2L_B\pi}{W}\right) + 2\cos\left(\frac{2\pi z}{W}\right)}{\cosh\left(\frac{2L_A\pi}{W}\right) + \cosh\left(\frac{2L_B\pi}{W}\right)} \tag{20}$$

takes the fingers located in between $(0, 0)$ and $(0, iL_A)$ and $(W/2, 0)$ and $(W/2, W/2 + iL_B)$ to a line segment extending from $(-1, 0)$ to $(1, 0)$ (note that there is a mistake in the mapping quoted in [21]). The potential around such a line segment is

$$u(w) = \frac{W}{2\pi}\operatorname{arc\,cosh} w \tag{21}$$

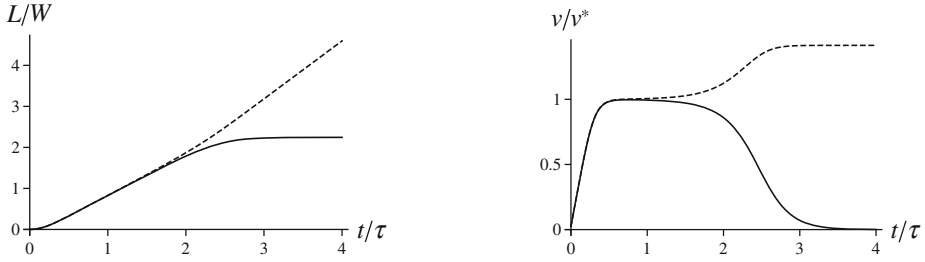

Fig. 9. The evolution of two Laplacian fingers: lengths (left) and growth velocities (right) vs time. The solid line represents the shorter finger (A), whereas the longer one (B) is represented by the dashed line. Velocity is rescaled by v^*, defined in Eq. (25). Time is rescaled by a factor of $\tau = W/v^*$

Combining the above results, we obtain the pressure field around the two fingers as $p(z) = u(w(z))$, with $z = X + iY$. Note that the prefactor in (21) has been chosen in this form $(W/2\pi)$ in order to guarantee a proper asymptotic behavior of p as $y \to \infty$. Next, the coefficients C_i in (18) can be obtained as

$$C_i = \lim_{\epsilon \to 0} \frac{p(\gamma_i + \epsilon \mathbf{e}_Y)}{\sqrt{\epsilon}} \tag{22}$$

where γ_i denotes the position of the tip of ith finger. This procedure leads to:

$$C_i = \sqrt{\frac{2W}{\pi}} \sqrt{\frac{\sinh \frac{2L_i\pi}{W}}{\cosh \frac{2L_A\pi}{W} + \cosh \frac{2L_B\pi}{W}}} \tag{23}$$

and, based on (19)

$$v_i = v^* \sqrt{\frac{2\sinh \frac{2L_i\pi}{W}}{\cosh \frac{2L_A\pi}{W} + \cosh \frac{2L_B\pi}{W}}} \tag{24}$$

where

$$v^* = \frac{1}{\rho s} \sqrt{\frac{2W}{\pi l}} \,. \tag{25}$$

A typical evolution of the finger lengths is presented in Fig. 9. At the initial stage, the fingers almost do not interact, their velocities increase quickly but remain equal to each other. Then, as the length of the fingers becomes comparable to the system size, their velocities stabilize at $v_A = v_B = v^*$, which can be obtained from Eq. (24) by imposing $L_A = L_B$ and taking the limit $L_A/W, L_B/W \to \infty$. At that point, however, the fingers begin to compete with each other, which is accompanied by a sharp decrease of the velocity of the losing finger and the corresponding increase of velocity of the winning one up to the asymptotic value ($v_B = \sqrt{2}v^*$), which again can be recovered from Eq. (24), this time by taking the limit $L_A/W \to 0, L_B/W \to \infty$.

In the case of two Laplacian fingers considered above, the explicit form of $G(x, y)$ may be found in the regime when the finger lengths are longer then the system width, $L \gg W$. The hyperbolic functions in (23) can then be approximated by exponentials and the function G reads

$$G(x, y) = \frac{(x-1)x(2x-1)\log\left(\frac{1}{x} - 1\right)}{(2(x-1)x+1)(2y-1)} \,. \tag{26}$$

The phase space trajectories in this case are presented in the right panel of Fig. 8. As expected, both $(0, 0)$ and $(1/2, 1/2)$ are equilibrium points of the dynamics.

The analysis of the phase space flow in vicinity of those points is hindered since the partial derivatives of $G(x, y)$ diverge there. Nevertheless, the character of the motion can be assessed by a direct solution of the equations of motion near the fixed points. For example, near $(0, 0)$ one gets

$$\frac{dx}{dt} = x \log x \tag{27}$$

$$\frac{dy}{dt} = x - y \tag{28}$$

which can be integrated to yield

$$x = x_0^{e^t} \tag{29}$$

$$y = y_0 e^{-t} + \frac{e^{-t}}{\log x_0}(x_0^{e^t} - x_0) \tag{30}$$

which shows that $(x, y) \to (0, 0)$, so it is indeed a stable fixed point. The stable manifolds are directed along the $(0, 1)$ and $(1, 0)$ respectively.

On the other hand, the dynamics in the vicinity of $(1/2, 1/2)$ is governed by

$$\frac{dx'}{dt} = 2(x')^2/y \tag{31}$$

$$\frac{dy'}{dt} = x' - y' \tag{32}$$

where $x' = x - 1/2$ and $y' = y - 1/2$. This time, there is an unstable manifold tangent to $(-1, 0)$, whereas the stable direction is along $(1, 0)$. Therefore, this point is a saddle point.

6 Summary

In this paper we have studied the growth and competition of thin-and-long viscous fingers. It has proved convenient to track their dynamics in the variables corresponding to their relative velocities and lengths. In such a phase space, there were generally two fixed points – one corresponding to the case where both fingers have equal length and the other – when the growth of the shorter one is screened by the longer one. The first fixed point has been shown to be unstable, even for the independently growing fingers of Fig. 5. The second point is stable and is located either at $(0, 0)$ (for the infinite viscosity ratio) or at some finite (x_f, y_f) for the finite viscosity ratio. In the latter case the screening is incomplete, and the velocity of the shorter finger approaches a constant value in the long-time limit. Two different models for the interacting fingers have been considered: in the first, the interaction was mediated by two connectors only; in the second, the fingers were taken to be immersed in a rectangular cell filled with the viscous fluid. Surprisingly, the geometry of the phase space flow turned out to be remarkably similar in both cases. This confirms the hypothesis that the flow-capturing mechanism is indeed one of the main driving factors in finger evolution.

This work was supported by the National Science Centre (Poland) under research Grant No. 2012/07/E/ST3/01734. A.B. acknowledges the support of the Foundation for Polish Science (FNP) through the TEAM/2010-6/2 project cofinanced by the EU European Regional Development Fund. The experiments on viscous fingering in microfluidic channels were conducted together with Piotr Garstecki and Adam Samborski from the Institute of Physical Chemistry, Polish Academy of Sciences, who are gratefully acknowledged. We also benefited from discussions with Tony Ladd on the nature of finger-finger interaction in nonequilibrium growth systems.

References

1. R.A. Wooding, J. Fluid. Mech. **39**, 477 (1969)
2. G. Homsy, Annu. Rev. Fluid Mech. **19**, 271 (1987)
3. G. Menon, J. Non-Newton. Fluid Mech. **152**, 113 (2008)
4. R. Booth, J. Fluid Mech. **655**, 527 (2010)
5. G. Rousseaux, M. Martin, A. De Wit, J. Chromatogr. A **1218**, 8353 (2011)
6. A. Budek, P. Garstecki, A. Samborski, P. Szymczak, J. Fluid. Mech. (submitted) (2014)
7. J.D. Chen, D. Wilkinson, Phys. Rev. Lett. **55**, 1892 (1985)
8. E. Ben-Jacob, R. Godbey, N. Goldenfeld, J. Koplik, H. Levine, T. Mueller, L. Sander, Phys. Rev. Lett. **55**, 1315 (1985)
9. J.D. Chen, Exp. Fluids **5**, 363 (1987)
10. V. Horváth, T. Vicsek, J. Kertész, Phys. Rev. A **35**, 2353 (1987)
11. P. Kelemen, J. Whitehead, E. Aharonov, K. Jordahl, J. Geophys. Res. **100**, B475 (1995)
12. P. Szymczak, A.J.C. Ladd, J. Geophys. Res. **114**, B06203 (2009)
13. S. Curtis, J. Maher, Phys. Rev. Lett. **63**, 2729 (1989)
14. C.N. Baroud, S. Tsikata, M. Heil, J. Fluid Mech. **546**, 285 (2006)
15. Y. Couder, F. Argoul, A. Arnéodo, J. Maurer, M. Rabaud, Phys. Rev. A **42**, 3499 (1990)
16. Y. Couder, J. Maurer, R. González-Cinca, A. Hernández-Machado, Phys. Rev. E **71**, 31602 (2005)
17. T.C. Halsey, M. Leibig, Phys. Rev. A **46**, 7723 (1992)
18. T.C. Halsey, Phys. Rev. Lett. **46**, 1228 (1994)
19. Y. Sawada, A. Dougherty, J. Gollub, Phys. Rev. Lett. **56**, 1260 (1986)
20. P. Szymczak, A.J.C. Ladd, Geophys. Res. Lett. **33**, L05401 (2006)
21. J. Krug, K. Kessner, P. Meakin, F. Family, Europhys. Lett. **24**, 527 (1993)